
WHERE TO DRILL NEXT? A DUAL-WEIGHTED APPROACH TO ADAPTIVE OPTIMAL DESIGN OF GROUNDWATER SURVEYS

A PREPRINT

Mikkel B. Lykkegaard*

Centre for Water Systems and
Institute for Data Science and AI
University of Exeter
Exeter, EX44QF
m.lykkegaard@exeter.ac.uk

Tim J. Dodwell

The Alan Turing Institute and
Institute for Data Science and AI
University of Exeter
Exeter, EX44QF
tdodwell@turing.ac.uk

February 25, 2022

ABSTRACT

We present a novel approach to adaptive optimal design of groundwater surveys – a methodology for choosing the location of the next monitoring well. Our dual-weighted approach borrows ideas from Bayesian Optimisation and goal-oriented error estimation to propose the next monitoring well, given that some data is already available from existing wells. Our method is distinct from other optimal design strategies in that it does not rely on Fisher Information and it instead directly exploits the posterior uncertainty and the expected solution to a dual (or *adjoint*) problem to construct an acquisition function that optimally reduces the uncertainty in the model as a whole and some engineering quantity of interest in particular. We demonstrate our approach in the context of 2D groundwater flow example and show that the dual-weighted approach outperforms the baseline approach with respect to reducing the error in the posterior estimate of the quantity of interest.

Keywords Adaptive Optimal Design · Groundwater Surveying · Uncertainty Quantification · Bayesian Inverse Problems · Adjoint State Equations

*Corresponding author.

1 Introduction

In this paper, we present a novel approach to optimally choosing the location of the next monitoring well when conducting a groundwater survey. Establishing a monitoring well is generally costly, and depends on the specific geological context and the required penetration depth, and choosing the most informative location for each well is a critical task when designing a groundwater survey. Groundwater surveying and modelling are intrinsically imbued with uncertainty and solutions and predictions are without exception non-unique [1]. Hence, in this paper we assume the perspective that a useful sampling location is one that most significantly reduces the uncertainty in the solution, while simultaneously having a substantial influence on some quantity of interest (QoI). While multiple non-invasive and relatively inexpensive methods for groundwater surveying exist [2, 3, 4, 5], these methods all involve solving an inverse problem to reconstruct the hydraulic head, which introduces an additional layer of uncertainty. Hence, in this work, we focus on the problem of determining aquifer characteristics from direct point measurements of hydraulic head and flux from monitoring wells, and how to optimally choose the locations of such wells, given existing data. While the method is here contextualised within this particular problem, it can easily be generalised to any setting where a continuous function and a derived QoI are approximated with point measurements.

In the “classic” theory of optimal design, we often distinguish between optimality criteria that minimise the estimated parameter variances (e.g. A –, D – and E –optimality) and those that minimise the prediction variance (e.g. G –, V – and I –optimality) [6, 7]. Since in this study we are primarily concerned with the prediction variance, the method presented here belongs in the latter category. In this context, our method can broadly be considered G –optimal, since our vanilla acquisition function targets the location of the highest posterior dispersion [see e.g. 7]. However, rather than iteratively searching for a design that maximises an optimality criterion, we directly utilise a posterior dispersion estimate to construct an acquisition function. We remark that while there are some abstract parallels between the method presented here and classic optimal design, our method is probably better understood in the context of Bayesian Optimisation, as discussed later. Additionally, the classic optimal design approach is typically centered around the problem of choosing an experimental design that is optimal with respect to an optimality criterion, *before taking any measurements*. In this paper, we take an adaptive approach and assume that some measurements are already available, and we want to propose optimal *new* sampling locations, given the data we already have. How the initial measurement locations are optimally chosen is beyond the scope of this paper, but we refer to e.g. Cox and Reid [8], Pukelsheim [6], Myers et al. [7] for an extensive overview of optimal design of experiments. We remark that our dual-weighted method could in theory be employed to choose initial measurement locations, but in that case the dispersion of the solution would be constrained only by the prior distribution of parameters and the constraints imposed by the constitutive equations. In this case, the method presented herein may be used in conjunction with some space-filling design strategy or using local penalisation functions as described in Section 2.3.2. However, either of these workarounds would require an informed prior to work well.

We recycle the notion from classic optimal design that the information gain is driven by minimising the dispersion of a target distribution [9]. However, rather than integrating out all possible measurements and model parameters to find the utility of a given design, we take a simpler approach. Namely, we use a Monte Carlo estimate of the (current) posterior dispersion of the solution to a Partial Differential Equation (PDE) (or some appropriate function thereof) as an acquisition function. The underlying rationale being that if we wish to know more about the distribution of our solution, the most useful place to take a new sample is at the point of the highest posterior uncertainty.

In this context, our Vanilla approach (see Section 2.3.1) is not dissimilar to the maximum entropy approach to the optimal sensor placement problem [10], where sensors are added at the point of the highest uncertainty of some probabilistic function that is fitted to current sensor measurements, for example a Gaussian Process (GP) emulator. While this strategy will typically place many sensors at the boundaries of the sampling space in the context of adaptive GP fitting [11], this is not necessarily the case when targeting the uncertainty of the solution to a PDE, since that will be constrained by boundary conditions. The sensor placement problem has been studied extensively in the context of GP emulators, and multiple improvements to the maximum entropy approach have been made (see e.g. Krause et al. [12], Beck and Guillas [13], Mohammadi et al. [11]). However, since our objective is to minimise the uncertainty of a PDE-derived QoI, and not a GP emulator, many of the recent developments are not immediately applicable, since they are tailored for use with a GP emulator. Hence, the Vanilla approach presented herein can be considered a reformulation of the original maximum entropy approach, particularly tailored for the (probabilistic) solution of a PDE.

Our method (see Section 2.3) borrows ideas from other fields, not obviously related to classic optimal design. First, our adaptive optimal design approach is formulated in terms of an acquisition function, a term typically associated with Bayesian Optimisation (BO, Moćkus [14], Frazier [15]). Moreover, our approach uses ideas from both prior-guided BO [16] and batch BO [17], the similarities with which are discussed in Section 2.3.3. While in the context of BO, the aim is to find the maximum or minimum of some function that is expensive to evaluate, our objective is to simply reduce the uncertainty of our model predictions. Hence, our vanilla acquisition function addresses solely the uncertainty of some target function, and not the function value itself. Second, our approach is inspired by the goal-oriented error-estimation used in mesh-adaptation for PDEs [18, 19], where the intention is to refine a mesh locally and parsimoniously to reduce the simulation error with respect to some QoI using an influence function that is the solution to an adjoint PDE. This approach, however, is most useful for forward problems, where the domain and coefficients are well-known, and the groundwater flow problem is typically not of this kind. Instead, we use the same approach of computing an influence function with respect to the QoI to determine, not where the mesh should be refined, but from where we need more data.

The idea of exploiting the adjoint or *dual* problem to minimise the posterior uncertainty with respect to a QoI was first explored by Attia et al. [20] in a similar context as our model problem. However, there are several crucial differences between their approach and the one presented in this paper. First, their method is set in the “classic” optimal design context, where a number of sampling locations

are determined before taking any measurements, based on the maximising the expected information gain according to some criterion derived from the Fisher Information matrix. Second, since only a finite number of designs can be explored this way, the prospective sampling locations are fixed to a relatively coarse grid. Finally, the approach described in Attia et al. [20] requires the adjoint operator to be linear – an assumption which is suitable for only a subset of QoIs.

We employ Markov Chain Monte Carlo (MCMC) techniques (see Section 2.1) to generate samples from the posterior distribution of the model parameters given the data $\pi(\theta|\mathbf{d})$, where the model parameters (θ) in this case describe hydraulic conductivity and the data (\mathbf{d}) are point measurements of hydraulic head and flux (see Section 2.2). Even if the model parameters themselves are of secondary interest to a given problem, we can use the MCMC samples to construct Monte Carlo estimates of any parameter-derived quantity or function, such as the hydraulic flux across a boundary, or the peak concentration of a contaminant at a well. Additionally, unlike traditional inversion techniques, MCMC allows for rigorously quantifying the uncertainty of the inverse problem, which is useful in the context of engineering decision support systems, in particular risk assessment studies. We believe that there are many unexploited application opportunities tangential to the study of Bayesian posteriors and demonstrate, in this paper, one such application.

Figure 1 illustrates the proposed workflow at a high level, where new wells are sequentially established at locations of high uncertainty and influence on a QoI, as dictated by the acquisition function. This paper is mainly concerned with the construction of optimal acquisition functions based on the posterior information which would be immediately available from quantifying the uncertainty of the Bayesian inverse problem.

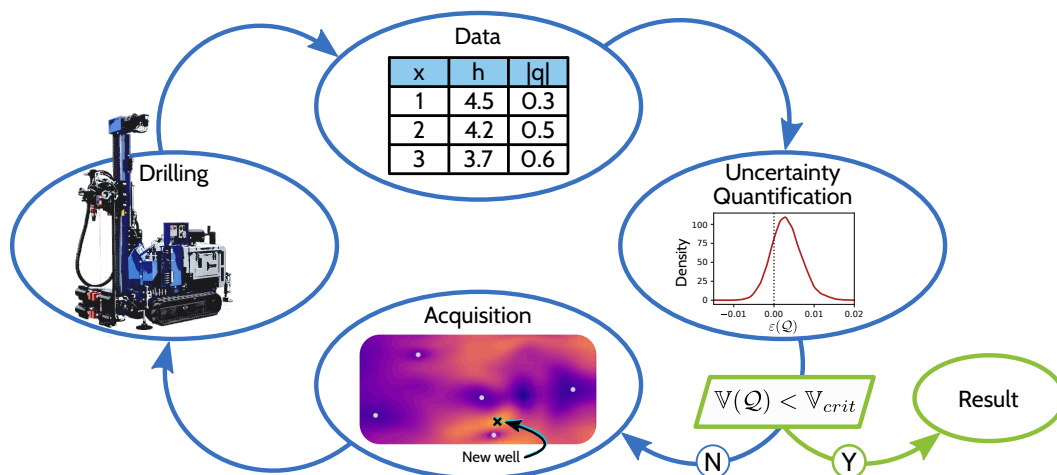


Figure 1: Conceptual diagram of the proposed adaptive optimal design workflow. Here, $\mathbb{V}(Q)$ denotes the variance of the quantity of interest Q and \mathbb{V}_{crit} the desired critical variance.

In the following sections, we briefly summarise the theory of Bayesian inverse problems, MCMC and groundwater flow modelling. We then outline the proposed methodology and demonstrate the effectiveness of methodology on a synthetic example. We show that efficient acquisition functions

can easily be constructed from information that would already be available from solving the Bayesian inverse problem using MCMC. The method avoids many of the complex calculations that are associated with classic optimal design and exploits information about the Bayesian posterior in a direct and straightforward way.

2 Theory

In this section, we first briefly outline the framework of Bayesian inverse problems and Markov Chain Monte Carlo (MCMC), a popular technique employed to draw samples from the Bayesian posterior. We then summarise the fundamentals of groundwater flow modelling for steady-state groundwater flow in a confined aquifer using the Finite Element Method (FEM). Finally, we describe our novel approach to adaptive optimal design of groundwater surveys.

2.1 Bayesian Inversion

A Bayesian inverse problem can be stated compactly as: Given some data \mathbf{d} , find the distribution $\pi(\theta|\mathbf{d})$ with model parameters $\theta \in \Theta$, where Θ is the parameter space, so that

$$\mathbf{d} = \mathcal{F}(\theta) + \epsilon \quad (1)$$

where $\mathcal{F}(\theta)$ is the model output and ϵ is the measurement error, which is typically assumed to be Gaussian. Bayes theorem then states that

$$\pi(\theta|\mathbf{d}) = \frac{\pi_p(\theta)\mathcal{L}(\mathbf{d}|\theta)}{\pi(\mathbf{d})} \quad (2)$$

where $\pi(\theta|\mathbf{d})$ is referred to as the *posterior* distribution, $\pi_p(\theta)$ is *prior* distribution, encapsulating what we already know about our model parameters and $\mathcal{L}(\mathbf{d}|\theta)$ is called the *likelihood*, essentially a measure of misfit between the model output $\mathcal{F}(\theta)$ and the data \mathbf{d} . While the the so-called *evidence* $\pi(\mathbf{d}) = \int_{\Theta} \pi_p(\theta) \mathcal{L}(\mathbf{d}|\theta) d\theta$ is generally infeasible or impossible to determine in most real-world scenarios, various sampling techniques allows us to make statistical inferences from $\pi(\theta|\mathbf{d})$ anyway. Examples include Importance Sampling (IS) and Markov Chain Monte Carlo (MCMC) methods. While these methods are not the object of this study, a short summary of the main ideas of MCMC, which is the specific method employed for inversion in this study, is provided for completeness.

In MCMC we exploit that $\pi(\mathbf{d})$ is constant and does not depend on the parameters θ . We can therefore write

$$\pi(\theta|\mathbf{d}) \propto \pi_p(\theta)\mathcal{L}(\mathbf{d}|\theta) \quad (3)$$

or equivalently, for $x, y \in \Theta$

$$\frac{\pi(y|\mathbf{d})}{\pi(x|\mathbf{d})} = \frac{\pi_p(y)\mathcal{L}(\mathbf{d}|y)}{\pi_p(x)\mathcal{L}(\mathbf{d}|x)} \quad (4)$$

We then introduce a *transition kernel* or *proposal distribution* $q(y|x)$, allowing us to transition from one state x to another y . Repeatedly applying the transition kernel $q(y|x)$ followed by an accept/reject step prescribed by equation (5) we construct a Markov chain where the samples, after an initial *burn-in*, are precisely from the required distribution $\pi(\theta|\mathbf{d})$. Here, burn-in refers to the initial MCMC samples which are discarded, since they may not be representative of the equilibrium distribution of the Markov chain. This procedure is described in the box below [21, 22, 23].

The Metropolis-Hastings Algorithm, $\theta^{(0)} \sim \pi_p(\theta)$, for $i = 0, \dots, N$:

1. Given a parameter realisation $\theta^{(i)}$ and a transition kernel $q(\theta'|\theta^{(i)})$, generate a proposal θ' .
2. Compute the acceptance probability of the proposal given the previous realisation:

$$\alpha(\theta'|\theta^{(i)}) = \min \left\{ 1, \frac{\pi_p(\theta') \mathcal{L}(\mathbf{d}|\theta')}{\pi_p(\theta^{(i)}) \mathcal{L}(\mathbf{d}|\theta^{(i)})} \frac{q(\theta^{(i)}|\theta')}{q(\theta'|\theta^{(i)})} \right\} \quad (5)$$
3. If $u \sim U(0, 1) > \alpha$ then set $\theta^{(i+1)} = \theta^{(i)}$, otherwise, set $\theta^{(i+1)} = \theta'$.

The acceptance probability (Eq. 5) ensures that the algorithm is in detailed balance with the target (posterior) distribution $\pi(\theta|\mathbf{d})$. See e.g. Liu [24, Sec. 5.3] for more details. Note that when the measurement error ϵ is Gaussian, $\epsilon \sim \mathcal{N}(0, \Sigma_\epsilon)$, which we assume in the experiment in Section 3, then the (unnormalised) likelihood functional takes the following form:

$$\mathcal{L}(\mathbf{d}|\theta) \propto \exp \left(-\frac{1}{2} (\mathcal{F}(\theta) - \mathbf{d})^T \Sigma_\epsilon^{-1} (\mathcal{F}(\theta) - \mathbf{d}) \right). \quad (6)$$

In this study we employ a number of extensions to the Metropolis-Hastings algorithm to speed up inference, namely the Delayed Acceptance (DA, [25]) algorithm with finite subchains [26, 27], also referred to as the *surrogate transition method* by Liu [24]. The DA algorithm exploits an approximate forward model (or Reduced Order Model, ROM) $\hat{\mathcal{F}}$ to filter MCMC proposals before evaluating them with the fully resolved forward model \mathcal{F} , resulting in a reduction in computational cost. Moreover, we employ a state-independent Approximation Error Model (AEM) to probabilistically correct for model reduction errors introduced by the approximate model, as described by Cui et al. [28]. Finally, we use the Adaptive Metropolis (AM) algorithm as the transition kernel [29]. In this work, we used the open-source DA MCMC framework `tinyDA`[†] to perform the MCMC sampling.

2.2 Groundwater Flow

The groundwater flow equation for steady flow in a confined, inhomogeneous aquifer occupying the domain Ω with boundary Γ can be written as the scalar elliptic partial differential equation

$$-\nabla \cdot k(\mathbf{x}) \nabla u(\mathbf{x}) = g(\mathbf{x}), \quad \text{for all } \mathbf{x} \in \Omega, \quad (7)$$

[†]<https://github.com/mikkelbue/tinyDA>

subject to boundary conditions on $\Gamma = \Gamma_D \cup \Gamma_N$ with the constraints

$$u(\mathbf{x}) = u_D(\mathbf{x}) \quad \text{on } \Gamma_D \quad \text{and} \quad -(k(\mathbf{x})\nabla u(\mathbf{x})) \cdot \mathbf{n} = q_N(\mathbf{x}) \quad \text{on } \Gamma_N. \quad (8)$$

Here, $k(\mathbf{x})$ is the hydraulic conductivity, $u(\mathbf{x})$ is the hydraulic head, $g(\mathbf{x})$ are sources and sinks, and Γ_D and Γ_N are boundaries with Dirichlet and Neumann conditions, respectively (see e.g. Diersch [30]). If θ somehow parameterises the conductivity, then we have $k(\mathbf{x}) = k(\mathbf{x}, \theta)$. This equation can be converted into the weak form by multiplying with a test function $v \in H^1(\Omega)$ and integrating by parts:

$$\int_{\Omega} \nabla v \cdot (k(\mathbf{x}, \theta) \cdot \nabla u) \, d\mathbf{x} + \int_{\Gamma_N} v q_N(\mathbf{x}) \, ds = \int_{\Omega} v g(\mathbf{x}) \, d\mathbf{x}, \quad \forall v \in H^1(\Omega) \quad (9)$$

subject to the boundary condition $u(\mathbf{x}) = u_D(\mathbf{x})$ on Γ_D , where $H^1(\Omega)$ is the Hilbert space of weakly differentiable functions on Ω . We approximate the solution $u(\mathbf{x})$ in a finite element space $V_{\tau} \subset H^1(\Omega)$ on a finite element mesh $\mathcal{Q}_{\tau}(\Omega)$, defined by piecewise linear Lagrange polynomials $\{\phi_i(\mathbf{x})\}_{i=1}^M$ associated with the M finite element nodes. This can be rewritten as a sparse system of equations

$$\mathbf{A}(\theta)\mathbf{u} = \mathbf{b} \quad \text{where} \quad A_{ij} = \int_{\Omega} \nabla \phi_i(\mathbf{x}) \cdot k(\mathbf{x}, \theta) \nabla \phi_j(\mathbf{x}) \, d\mathbf{x} \quad \text{and} \quad (10)$$

$$b_i = - \int_{\Gamma_N} \phi_i(\mathbf{x}) q_N(\mathbf{x}) \, ds + \int_{\Omega} \phi_i(\mathbf{x}) g(\mathbf{x}) \, d\mathbf{x} \quad (11)$$

where $\mathbf{A}(\theta) \in \mathbb{R}^{M \times M}$ is the global stiffness matrix and $\mathbf{b} \in \mathbb{R}^M$ is the load vector. The solution to this system $\mathbf{u} := [u_1, u_2, \dots, u_M] \in \mathbb{R}^M$ represents the hydraulic head at each node, which can be interpolated to the entire domain using the finite element shape functions: $u(\mathbf{x}) = \sum_{i=1}^M u_i \phi_i(\mathbf{x})$. In our numerical experiments, we used the open-source high-performance finite elements package FEniCS [31] to solve these equations.

2.3 Adaptive Optimal Design

The overarching research question of this paper is this: if we want to collect more data to reduce the variance in our posterior Monte Carlo estimates, where in the modelling domain Ω should we do it, to maximise the benefit of the new borehole? More formally, if we let t denote the current design of the survey, so that \mathbf{d}_t and $\pi_t(\theta|\mathbf{d}_t)$ denote, respectively, the data and posterior distribution corresponding to that design, we want to find the next sampling point \mathbf{x}^* that constrains $\pi_{t+1}(\theta|\mathbf{d}_{t+1})$ in an optimal way, after setting $\mathbf{d}_{t+1} = (\mathbf{d}_t, d^*)^T$, where d^* is the newly collected data at \mathbf{x}^* .

2.3.1 “Vanilla” Approach

As outlined in section 2.1, Bayesian inversion allows us to construct the posterior distribution of parameters given the data $\pi_t(\theta|\mathbf{d}_t)$. If the inversion was completed using MCMC, and obtain-

ing the model output $\mathcal{F}(\theta)$ involved solving some partial differential equation with solution $u(\mathbf{x})$, we can cache these solutions during sampling, and would after sampling possess a set of pairs $\{(\theta^{(i)}, u^{(i)}(\mathbf{x}))\}_{i=0}^{N^\dagger}$. Since $\{\theta^{(i)}\}_{i=0}^{N^\dagger}$ are distributed exactly according to $\pi_t(\theta|\mathbf{d}_t)$, so are any functions of θ , such as $u(\mathbf{x})$. Here, N^\dagger is the number of MCMC samples after discarding the burn-in. Hence, we can easily obtain Monte Carlo estimates for

$$\mathbb{E}_{\pi_t(\theta|\mathbf{d}_t)}[u(\mathbf{x}, \theta)] \quad \text{and} \quad \mathbb{D}_{\pi_t(\theta|\mathbf{d}_t)}[u(\mathbf{x}, \theta)]$$

Here, \mathbb{D} signifies some measure of statistical dispersion, for example variance, standard deviation, or entropy. We could, in accordance with the maximum entropy approach [10], postulate that the accuracy of our inversion is driven by the dispersion in $u(\mathbf{x})$ and hence we could solve the following optimisation problem

$$\mathbf{x}^* = \arg \max_{\mathbf{x} \in \Omega} \mathbb{D}_{\pi_t(\theta|\mathbf{d}_t)}[u(\mathbf{x}, \theta)] \quad (12)$$

2.3.2 Dual-Weighted Approach

The simple approach outlined above will improve the general quality of $u(\mathbf{x})$, but it is limited by the fact that it is not tailored for a particular quantity of interest \mathcal{Q} and this is where the *dual weighted* approach comes into play. In this context, rather than simply sampling from places with high uncertainty, we aim to pick sampling points that also have a high expected influence on our quantity of interest \mathcal{Q} . This is exactly the problem, that *adjoint* or *dual* state methods aim to solve [32].

Suppose in a particular application, we are interested in estimating a particular quantity of interest $\mathcal{Q}(u)$, which we can write as a functional of the solution. For example, if our quantity of interest is the hydraulic head around a point $\mathbf{x}' \in \Omega$, we could choose

$$\mathcal{Q}_{\mathbf{x}'}(u) = \int_{\Omega} u(\mathbf{x}) \exp\left(-\frac{(\mathbf{x} - \mathbf{x}')^2}{\lambda}\right) d\mathbf{x} \quad (13)$$

for some sufficiently small length scale λ . This, however, is a trivial problem, since if the quantity of interest is the hydraulic head at some point, we can just place our monitoring well at that point and measure it. It would be much more useful to target a quantity of interest that we cannot measure directly. Hence, in this study we consider flux over a boundary Γ' with the following functional:

$$\mathcal{Q}_{\Gamma'}(u) = \int_{\Gamma'} [-k(\mathbf{x}, \theta) \cdot \nabla u(\mathbf{x})] \cdot \mathbf{n} ds \quad (14)$$

The adjoint state equation associated with Eq. (14) is

$$\nabla \cdot k \nabla \omega = 0 \quad (15)$$

subject to the boundary conditions

$$\begin{aligned} \omega_D(\mathbf{x}) &= 0 && \text{on } \Gamma_D \setminus \Gamma' \\ \omega_{\Gamma'}(\mathbf{x}) &= 1 && \text{on } \Gamma' \\ q_N^\omega(\mathbf{x}) &= (k(\mathbf{x})\nabla\omega(\mathbf{x})) \cdot \mathbf{n} = 0 && \text{on } \Gamma_N. \end{aligned}$$

The solution $\omega(\mathbf{x})$ is called the adjoint state or *influence* function. Please refer to Sykes et al. [33] and A for details on the derivation of the adjoint state equation and its associated boundary conditions. Integrating by parts and multiplying with a test function $v \in H^1(\Omega)$, we arrive at the weak form of the adjoint state equation:

$$\int_{\Omega} \nabla v \cdot (k(\mathbf{x}, \theta) \cdot \nabla \omega) d\mathbf{x} + \int_{\Gamma_N} v q_N^\omega(\mathbf{x}) ds = 0, \forall v \in H^1(\Omega) \quad (16)$$

subject to boundary conditions $\omega_D(\mathbf{x}) = 0$ on $\Gamma_D \setminus \Gamma'$ and $\omega_{\Gamma'}(\mathbf{x}) = 1$ on Γ' . Given some conductivity parameters θ , (16) can be discretised using the same finite element grid as (10), leading to the following sparse system of equations:

$$\mathbf{A}(\theta)\omega = \mathbf{b}_\omega \quad \text{where} \quad A_{ij} = \int_{\Omega} \nabla \phi_i(\mathbf{x}) \cdot k(\mathbf{x}, \theta) \nabla \phi_j(\mathbf{x}) d\mathbf{x} \quad \text{and} \quad (17)$$

$$b_{\omega,i} = - \int_{\Gamma_N} \phi_i(\mathbf{x}) q_N^\omega(\mathbf{x}) ds. \quad (18)$$

It is important to note here, that the stiffness matrix $\mathbf{A}(\theta)$, since the steady-state groundwater flow equation is *self-adjoint*, is exactly the same as in equation (10), and the assembled system can hence be partially recycled when solving both equations. However, since the boundary conditions for the adjoint state equation are different than for the primal problem, care must be taken when assembling the adjoint system of equations. After solving this system of equations, the influence function can be interpolated to the entire domain using our finite element shape functions:

$$\omega(\mathbf{x}) = \sum_{i=1}^M \omega_i \phi_i(\mathbf{x}) \quad \text{where} \quad \omega = [\omega_1, \omega_2, \dots, \omega_M]^T.$$

The influence function is commonly interpreted as the sensitivity of the quantity of interest to a unit point source anywhere on the domain [33, 34], or in this particular case as the sensitivity of flow anywhere on the domain to the boundary condition. Broadly speaking, the influence function directs us towards areas of the modelling domain with a potentially high influence on our quantity of interest, which is what we required for our dual-weighted approach.

We note that $\omega(\mathbf{x})$ is now a random function which depends on model parameters θ , and we can obtain estimates for $\mathbb{E}_{\pi_t(\theta|\mathbf{d}_t)}[\omega(\mathbf{x}, \theta)]$. Hence, we propose the following acquisition function

$$\mathbf{x}^* = \arg \max_{\mathbf{x} \in \Omega} \mathbb{D}_{\pi_t(\theta|\mathbf{d}_t)}[u(\mathbf{x}, \theta)] \cdot |\mathbb{E}_{\pi_t(\theta|\mathbf{d}_t)}[\omega(\mathbf{x}, \theta)]|. \quad (19)$$

where $|\cdot|$ denotes the absolute value. We use the absolute value of the expectation of the influence function to make sure that the weighting is always positive, since $\omega(\mathbf{x}, \theta)$ is not always positive for other adjoint equations. We call this approach dual-weighted, since we are essentially re-weighting the dispersion $\mathbb{D}_{\pi_t(\theta|\mathbf{d}_t)}[u(\mathbf{x}, \theta)]$, by the expected solution of the dual problem. Figure 2 illustrates the different steps in the proposed adaptive optimal design procedure.

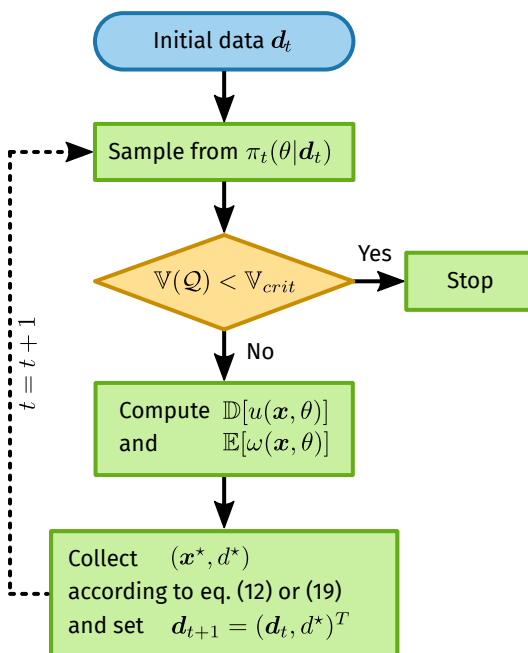


Figure 2: Proposed adaptive optimal design procedure. As in Figure 1, $\mathbb{V}(\mathcal{Q})$ denotes the variance of the quantity of interest \mathcal{Q} and \mathbb{V}_{crit} the desired critical variance.

2.3.3 Remarks

(1) The dual-weighted approach can be considered a hybrid between the goal-oriented error estimation employed for mesh-adaptation in the context of various expensive and mesh-sensitive PDE problems (see e.g. Prudhomme and Oden [18], Oden and Prudhomme [19]), and Bayesian Optimisation (BO), typically used to optimise some unknown function approximated with sparse and/or noisy data (see e.g. Moćkus [14], Frazier [15]). In this context, our dual-weighted approach could be framed as a form of prior-guided BO [16], where $\omega(\mathbf{x})$ broadly represents our prior belief that any point \mathbf{x}

constitutes a ‘‘good’’ sampling location. However, we remark that in our formulation $\omega(\mathbf{x})$ is not a probability distribution but a random weighting function.

(2) In the above formulations, we have chosen the dispersion of the hydraulic head $\mathbb{D}_{\pi_t(\theta|\mathbf{d}_t)}[u(\mathbf{x}, \theta)]$ as the function representing uncertainty in the model. Other sensible choices of uncertainty metrics would be the dispersion of the hydraulic conductivity $\mathbb{D}_{\pi_t(\theta|\mathbf{d}_t)}[k(\mathbf{x}, \theta)]$, or of some norm of the flux $\mathbb{D}_{\pi_t(\theta|\mathbf{d}_t)}[\|\mathbf{q}(\mathbf{x}, \theta)\|_p]$.

(3) Since sampling from $\pi_t(\theta|\mathbf{d}_t)$ can be computationally expensive, it may be desirable to pick multiple new sampling locations at each step of the algorithm. Denote the number of new sampling locations in each such batch acquisition as N^* . Then this can be achieved by penalising the acquisition function by some local penalisation functions $\{\psi_{\mathbf{x}_i^*}(\mathbf{x})\}_{i=1}^{N^*-1}$, centered on the previous sampling points $\{\mathbf{x}_i^*\}_{i=1}^{N^*-1}$ of the current batch, as described in Gonzalez et al. [17]. This approach would yield the following dual-weighted batch acquisition function for $\{\mathbf{x}_i^*\}_{i=2}^N$:

$$\mathbf{x}_i^* = \arg \max_{\mathbf{x} \in \Omega} \mathbb{D}_{\pi_t(\theta|\mathbf{d}_t)}[u(\mathbf{x}, \theta)] \cdot |\mathbb{E}_{\pi_t(\theta|\mathbf{d}_t)}[\omega(\mathbf{x}, \theta)]| \cdot \prod_{j=1}^{i-1} \psi_{\mathbf{x}_j^*}(\mathbf{x}). \quad (20)$$

Similarly, the batch acquisition function for the vanilla approach takes the form

$$\mathbf{x}_i^* = \arg \max_{\mathbf{x} \in \Omega} \mathbb{D}_{\pi_t(\theta|\mathbf{d}_t)}[u(\mathbf{x}, \theta)] \cdot \prod_{j=1}^{i-1} \psi_{\mathbf{x}_j^*}(\mathbf{x}). \quad (21)$$

A reasonable choice of penalisation functions would be the Gaussian

$$\psi_{\mathbf{x}'}(\mathbf{x}) = 1 - \exp\left(-\frac{1}{2} \frac{\|\mathbf{x} - \mathbf{x}'\|_2^2}{l_\psi}\right) \quad (22)$$

where l_ψ controls the dispersion of the function and $\|\cdot\|_2$ is the L^2 -norm. Using such a penalisation function, the acquisition function would be exactly zero at previous sampling points from the current batch, and smoothly rebound to Eq. (19) or Eq. (12) as the distance to previous sampling points increases.

(4) As mentioned earlier, we formulate our method in the context of steady state groundwater flow in a confined aquifer. While this is the most common approach to groundwater flow modelling, it is, naturally, not exhaustive. For a detailed analysis of the adjoint state equations for transient groundwater flow, we refer the to e.g. Sun [35] and Lu and Vesselinov [36]. The unconfined case is considerably more complex, since the constitutive equations are nonlinear. While unconfined groundwater flow can, under some assumptions, be reasonably approximated by the constitutive equations for confined flow [37], this is not always the case. For a derivation and analysis of the adjoint equations pertaining to unconfined and coupled aquifers, we refer to e.g. Sun [35] and Neupauer and Griebing [38].

(5) Note that the constitutive and adjoint equations are discretised using FEM in the above section. We restrict ourselves to this method for brevity, but remark that the proposed acquisition functions

(Eqs. (12), (19), (20) and (21)) are valid for any discretisation scheme. Also note that if piecewise linear shape functions are employed to approximate $u(\mathbf{x})$, the maxima of the acquisition functions will occur at finite element nodes.

3 Example

In this section, we demonstrate the vanilla and dual-weighted approach in the context of a synthetic groundwater flow example. We first outline the model setup, including the geological model and finite element representation. We then explain the particular methodology for this example in detail. Finally, we present the results.

3.1 Model Setup

We model the hydraulic conductivity as a log-Gaussian Random Field with a Matern 3/2 covariance kernel:

$$C(\mathbf{x}, \mathbf{y}) = \left(1 + \sqrt{3} \frac{\|\mathbf{x} - \mathbf{y}\|_2}{l}\right) \exp\left(-\sqrt{3} \frac{\|\mathbf{x} - \mathbf{y}\|_2}{l}\right) \quad (23)$$

where l is the length scale [39] and $\|\cdot\|_2$ is the L^2 -norm. The resulting random field is expanded in an orthogonal eigenbasis with N_{KL} Karhunen–Loève (KL) eigenmodes. To this end, we construct a matrix of covariances between each pair of finite element nodes $\mathbf{C} \in \mathbb{R}^{M \times M}$ according to Eq. (23), so that $C_{ij} = C(\mathbf{x}_i, \mathbf{x}_j)$. This covariance matrix \mathbf{C} is decomposed into the N_{KL} largest eigenvalues $\{\lambda_i\}_{i=1}^{N_{\text{KL}}}$ and eigenvectors $\{\psi_i\}_{i=1}^{N_{\text{KL}}}$. The nodal conductivities $\mathbf{k} := [k_1, k_2, \dots, k_M]$ are then given by

$$\log \mathbf{k} = \mu + \sigma \Psi \Lambda^{\frac{1}{2}} \theta \quad (24)$$

with $\Lambda = \text{diag}([\lambda_1, \lambda_2, \dots, \lambda_{N_{\text{KL}}}]$) and $\Psi = [\psi_1, \psi_2, \dots, \psi_{N_{\text{KL}}}]$. The vector $\mu = \mu \mathbf{1}$ is the mean of the log-conductivity, σ is the standard deviation of the log-conductivity, and $\theta \sim \mathcal{N}(0, \mathbb{I}_{N_{\text{KL}}})$ [40]. When defined in this way, the associated Bayesian inverse problem involves exploring $\pi(\theta|\mathbf{d})$, i.e. the posterior distribution of hydraulic conductivity parameters θ given measurements \mathbf{d} , where the aforementioned normal distribution constitutes the prior distribution of parameters: $\pi_p(\theta) = \mathcal{N}(0, \mathbb{I}_{N_{\text{KL}}})$.

We used three different models for the experiments (Fig. 3), one *data-generating* model representing the ground truth, a *fine* forward model representing the fully resolved forward model \mathcal{F} in the Bayesian inverse problem (see Eq. (1)), and a *coarse* forward model, corresponding to the reduced order forward model in the Delayed Acceptance MCMC sampler $\hat{\mathcal{F}}$, as described in e.g. Christen and Fox [25], Liu [24], Cui et al. [28], Lykkegaard et al. [26, 27]. Note that using the dual-weighted approach described herein does not require a Delayed Acceptance MCMC sampler. Any method capable of producing Monte Carlo samples from the posterior will do.

The experiments were performed on a rectangular domain $\Omega = [0, 2] \times [0, 1]$ meshed using a structured triangular grid with $M_{\text{fine}} = 1326$ degrees of freedom for the data-generating model and the fine forward model, and $M_{\text{coarse}} = 703$ degrees of freedom for the coarse forward model.

For the data-generating model, the log-Gaussian random conductivity was truncated at $N_{\text{KL}} = 256$ KL eigenmodes, while for the fine and coarse models it was truncated at $N_{\text{KL}} = 128$. Hence the dimensionality of the inverse problem in these experiments was 128, which is very high and a challenging problem for any MCMC algorithm. Moreover, we set $l = 0.1$, $\mu = -2$ and $\sigma = 1.0$ for every model. This resulted in strongly anisotropic conductivity fields with log-conductivities broadly between -5 and 1 (Fig. 3a).

We imposed fixed head Dirichlet boundary conditions of 1 and 0 on the left and right boundaries, respectively, and no-flow Neumann conditions on the remaining top and bottom boundaries. We set the right hand side of Eq. (7) to $g(\mathbf{x}) = 0$. We chose flux across the right boundary Γ_r as our quantity of interest \mathcal{Q} , corresponding to the following functional (as in equation (14)):

$$\mathcal{Q}(u) = \int_{\Gamma_r} [-k(\mathbf{x}, \theta) \cdot \nabla u(\mathbf{x})] \cdot \mathbf{n} \, ds \quad (25)$$

and the associated adjoint state equation shown in (15) with $\Gamma' = \Gamma_r$. Figure 3f shows an example of the influence function generated by this adjoint state equation. The left column of Fig. 3 shows the conductivity associated with a random draw from the prior $\pi_p(\theta)$, for the data-generating model, the fine model, and the coarse model, respectively. The right column of Fig. 3 shows the corresponding hydraulic head, flux and influence function for the data-generating model.

3.1.1 Methodology

Using the above setup, we completed a total of $n = 30$ independent numerical experiments to demonstrate the feasibility of the dual-weighted approach. We chose the standard deviation of the L^2 -norm of the flux $S(\|\mathbf{q}(\mathbf{x})\|_2)$ as the general measure of uncertainty in the model. For each independent experiment, the following experimental procedure was observed: (1) The hydraulic conductivity for the data-generating model was initialised with a random draw from the prior, and the primary problem was solved. (2) Eight observation wells were placed randomly on the domain by Latin Hypercube sampling [41] (see Fig. 4). (3) For each observation well \mathbf{x}_i , the hydraulic head $u(\mathbf{x}_i)$ and the norm of the flux $\|\mathbf{q}(\mathbf{x}_i)\|_2$ were computed. These head and flux observations were contaminated with white noise from $\epsilon_u \sim \mathcal{N}(0, 0.01^2)$ and $\epsilon_{\|\mathbf{q}\|_2} \sim \mathcal{N}(0, 0.001^2)$, respectively. (4) Delayed Acceptance MCMC sampling was completed with 2 independent samplers each drawing $N = 25000$ fine samples with a subsampling length of 5 (see e.g. Lykkegaard et al. [26, 27]), and a burn-in of $N_{\text{burn}} = 5000$ was discarded. This resulted in a total number of MCMC samples of $N^\dagger = 40000$ for each experiment. (5) The standard deviation of the L^2 -norm of the flux $S(\|\mathbf{q}(\mathbf{x})\|_2)$ and the mean of the influence function $\bar{\omega}(\mathbf{x})$ were computed at the finite element nodes and interpolated to the entire domain using the finite element shape functions, and eight new observation wells were placed according to the batch vanilla and dual-weighted acquisition functions, see Eq. (21) and Eq. (20). Figure 4 shows the vanilla and dual weighted acquisition functions for one sample of the $n = 30$ models. As expected, the weighting function $\bar{\omega}(\mathbf{x})$ prioritised observation wells closer to the boundary of the quantity of interest. (6) Data were extracted from the four new observation wells as

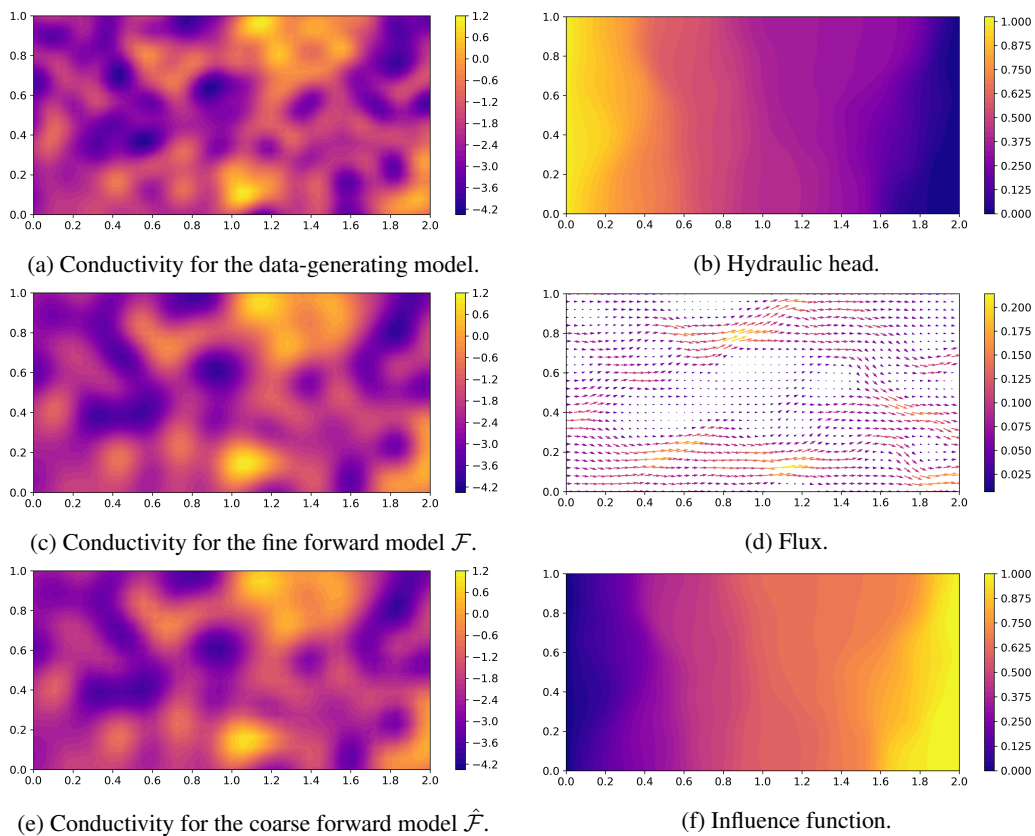


Figure 3: A random realisation from the prior $\pi_p(\theta)$, with the corresponding primary and adjoint solutions. The left column shows the conductivity for the data-generating model (a), the fine forward model (c) and the coarse forward model (e) respectively. The right column shows the hydraulic head (b), the flux (d), and the influence function (f), respectively.

in step (3) and appended to the data vector. (7) Delayed Acceptance MCMC sampling was repeated, using the new data vectors for both the vanilla and dual-weighted approaches.

For each experiment and each posterior distribution (initial, vanilla, and dual-weighted) with each $N^\dagger = 40000$ posterior samples, we computed the mean squared error (MSE) and variance of the predicted quantity of interest $\{Q^{(i)}\}_{i=1}^{N^\dagger}$ compared to the true value Q_{true} . The MSE of the predicted value of the quantity of interest $Q^{(i)}$ with respect to the true value Q_{true} was computed as

$$\text{MSE} = \frac{1}{N^\dagger} \sum_{i=1}^{N^\dagger} (Q_{true} - Q^{(i)})^2 \quad (26)$$

Similarly, the sample variance of Q for each experiment was computed as:

$$s^2 = \frac{1}{N^\dagger - 1} \sum_{i=1}^{N^\dagger} (Q^{(i)} - \bar{Q})^2 \quad (27)$$

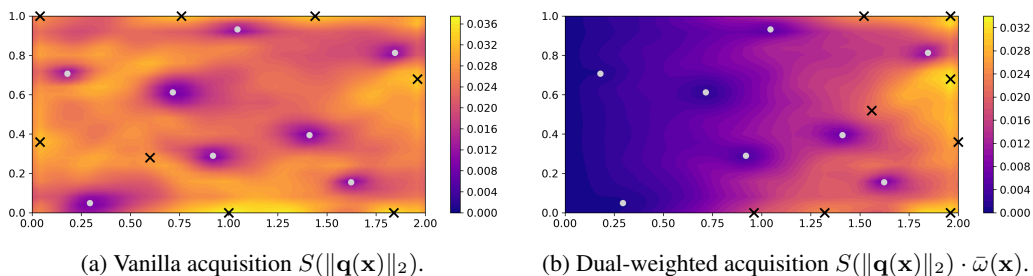


Figure 4: Acquisition functions of the vanilla and dual-weighted approaches for one sample of the $n = 30$ models. The white dots show the initial datapoints, while the black crosses show the new datapoints suggested by each acquisition function.

Finally, we constructed Gaussian kernel posterior density estimates $\hat{f}_{\pi(\theta|\mathbf{d})}(\mathcal{Q})$ from the posterior samples from each experiment $\{Q^{(i)}\}_{i=1}^{N^\dagger}$, and computed the kernel density of the true value Q_{true} with respect to this density estimate. Kernel density estimates were computed using SciPy [42] with automatic bandwidth determination [43].

3.1.2 Results

We compared the MSE, variance, and kernel density of both the vanilla and dual-weighted posterior samples with the corresponding values for the initial posterior samples for all $n = 30$ experiments.

With respect to the MSE, the vanilla approach yielded a median reduction of 22%, while the dual-weighted approach yielded a median reduction of 30% (Fig. 5a). This demonstrates that both acquisition strategies approach the true value when we add more datapoints, but that the dual-weighted approach is more efficient. With respect to the variance of the quantity of interest, the vanilla approach yielded a median reduction of 31%, while the dual-weighted approach yielded a median reduction of 34% (Fig. 5b). This shows that for both acquisition strategies the posterior distribution contracts as more data is added, and that the two approaches differ less with respect to this feature. However, this metric shows only that the posterior contracts, and not if it moves closer to the true value. Finally, we computed the posterior densities of the true quantity of interest with respect to kernel posterior density estimates $\hat{f}_{\pi(\theta|\mathbf{d})}(\mathcal{Q})$ for each experiment. Here, the vanilla approach yielded a median improvement of 12%, while the dual-weighted approach yielded a median improvement of 17%. Since the prediction variance of the quantity of interest reduced in every experiment (Fig. 5b), this again shows that the posterior distribution moves closer to the true value as more data is added, but that the dual-weighted approach is better.

We note that in neither method was capable of improving the posterior estimate of the quantity of interest for every experiment. Hence, in 8/30 vanilla experiments and 5/30 dual-weighted experiments, adding additional wells resulted in a worse posterior MSE than the initial one. This is not surprising since we are dealing with a very ill-posed inverse problem, and any new datapoint may reinforce the initial bias rather than reduce it. While both approaches occasionally failed to improve the posterior estimate, the dual-weighted approach performed better than the vanilla approach.

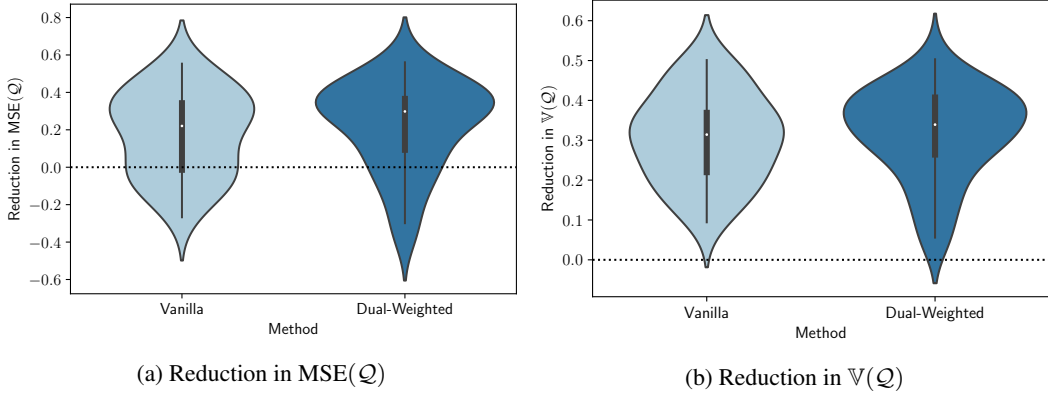


Figure 5: Kernel densities of the sample error of the quantity of interest $\varepsilon^{(i)} = Q_{true} - Q^{(i)}$ for the initial, vanilla and dual-weighted posteriors for two samples of the $n = 30$ experiments.

We computed the Gaussian kernel density estimates of the error $\varepsilon^{(i)} = Q_{true} - Q^{(i)}$ for two samples of the $n = 30$ experiments. The left panel shows a typical example, where the vanilla approach resulted in a moderate improvement while the dual-weighted approach yielded a more dramatic improvement. The right panel shows an example where both the dual-weighted and vanilla approaches failed to produce any improvement.

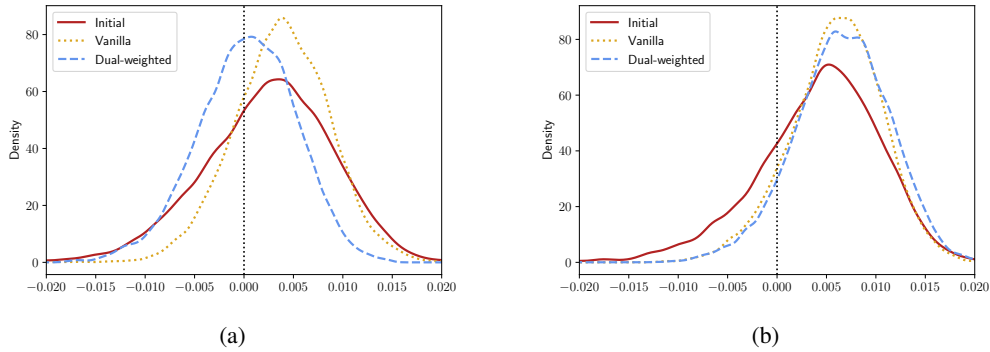


Figure 6: Kernel densities of the sample error of the quantity of interest $\varepsilon^{(i)} = Q_{true} - Q^{(i)}$ for the initial, vanilla and dual-weighted posteriors for two samples of the $n = 30$ experiments.

4 Discussion

In this paper, we have proposed a novel approach to the problem of optimally choosing the next location for a monitoring well, given existing data and some quantity of interest (QoI). The proposed methodology exploits the solution of an adjoint problem to weigh such an acquisition function according to the expected influence on the QoI. Numerical experiments have demonstrated that the approach works for our model problem. We emphasize that the problem is intrinsically probabilistic,

and hence subject to uncertainty. We have demonstrated that the approach works *on average* for our model problem, but there were certain experiments, where the dual-weighted acquisition strategy did not approach the true QoI (see e.g. Fig. 6b). As the number of wells approach infinity, the posterior distribution will certainly approach the true value, but for any one new observation well, there are no such guarantees. In a sense, the dual-weighted approach merely increases the chance of improving the posterior distribution of the QoI.

While we formulated and demonstrated the approach in the context of a groundwater surveying problem, the method could be applicable to other areas of science and engineering, where measurements are expensive. The most obvious parallel application is petroleum engineering, where there are similarities both in terms of the constituent equations and the mode of sampling, but the method could be adapted with little effort to any inverse problem where establishing sensors is expensive. We note, however, that the dual problem in our case was unusually simple, since the groundwater flow equation is self-adjoint. Clearly, the dual-weighted approach can only be used as-written for QoIs, where an adjoint problem can be formulated and solved directly. For more complicated QoIs, an alternative approach would be to perturb the posterior mean or mode to approximate the influence function. Using such an approach would yield $\omega(\mathbf{x}, \mathbb{E}[\theta])$ rather than $\mathbb{E}[\omega(\mathbf{x}, \theta)]$ as a weighting function.

A bottleneck of our approach is that the MCMC sampler is rerun after each (batch) data acquisition. Running MCMC for expensive forward models is notoriously computationally demanding, and while we employ various tricks to reduce the cost (such as Delayed Acceptance and proposal adaptivity), this is not the most elegant approach. One way to significantly alleviate the cost of subsequent posterior distributions would be to employ a particle filter to sequentially reweigh MCMC samples according to the new data [44]. This sequential approach was investigated in this study but it did not work well, mainly because of very high sample degeneracy. When the variance of the solution, as in our case, is relatively high at unobserved locations, only few posterior samples fit the new observations well, with the mentioned sample degeneracy as a result. Moreover, we found that the dispersion measures in Eqs. (12), (19), (20) and (21) were highly sensitive to this sample degeneracy. This challenge could be alleviated by drawing more posterior samples for the initial MCMC, but that would only offset the cost. We remark that this approach might work better for lower-dimensional problems than the one investigated in this study. We highlight this problem as a potential target for future research.

The methodology was demonstrated empirically in the context of a synthetic groundwater flow example. This gives rise to at least three additional interesting directions of future research. First, showing theoretically that the distribution of the quantity of interest does indeed converge faster to the true value when using the dual-weighted approach, and examining the mechanisms that govern this process in detail. Second, testing the method in practice in the context of an actual groundwater survey. While testing the method in practice would certainly expose limitations and complications that were not identified in this study, it would be difficult to validate the method further in this fashion, since the true value of the QoI is rarely known in reality. This may be overcome by testing the method

under controlled (laboratory) conditions. Third, generalising the dual-weighted approach to a wider range of PDE problems with different constituent equations and QoIs.

Acknowledgements

The MCMC code used for Delayed Acceptance sampling can be found at <https://github.com/mikkelbue/tinyDA>, and additional code will be made available in the Open Research Exeter data repository upon publication at <https://ore.exeter.ac.uk/repository/>. ML was funded as part of the Water Informatics Science and Engineering Centre for Doctoral Training (WISE CDT) under a grant from the Engineering and Physical Sciences Research Council (EPSRC), grant number EP/L016214/1. TD was funded by a Turing AI Fellowship (2TAFPP\100007). The authors would like to thank Robert Scheichl and Karina Koval for advice with regards to the formulation of the adjoint state equation. The authors have no competing interests.

Appendix A Adjoint State Equations

A.1 Domain Integral as Objective Function

Given an objective function defined as an integral over the entire domain

$$\mathcal{Q} = \int_{\Omega} f \, dx \quad (28)$$

Sykes et al. [33, Eq. (15)] write the derivative of \mathcal{Q} with respect to some parameter α as

$$\begin{aligned} \frac{d\mathcal{Q}}{d\alpha} = & \int_{\Omega} \left[\frac{\partial f}{\partial \alpha} + \psi \left(\frac{\partial f}{\partial u} + \nabla \cdot k \nabla \omega \right) + \omega \frac{\partial g}{\partial \alpha} - \nabla \omega \cdot \frac{\partial k}{\partial \alpha} \nabla u \right] dx \\ & + \int_{\Gamma} \left[\psi(k \nabla \omega) \cdot \mathbf{n} + \omega \frac{\partial q_N}{\partial \alpha} \right] ds \end{aligned} \quad (29)$$

To eliminate the unknown state sensitivities $\psi = \frac{\partial u}{\partial \alpha}$ they solve

$$\nabla \cdot k \nabla \omega + \frac{\partial f}{\partial u} = 0 \quad (30)$$

with boundary conditions $\omega_D = 0$ on Γ_D and $q_N^\omega = k \nabla \omega \cdot \mathbf{n} = 0$ on Γ_N .

A.2 Boundary Integral as Objective Function

The problem addressed in this paper involves an objective function defined on a fixed-head boundary Γ' :

$$\mathcal{Q} = \int_{\Gamma'} f \, ds \quad \text{with} \quad f = q = -k \nabla u \cdot \mathbf{n}^+ \quad (31)$$

Where \mathbf{n}^+ is the outward normal. Hence, the derivative of the objective function instead takes the form

$$\begin{aligned} \frac{dQ}{d\alpha} &= \int_{\Omega} \left[\psi (\nabla \cdot k \nabla \omega) + \omega \frac{\partial g}{\partial \alpha} - \nabla \omega \cdot \frac{\partial k}{\partial \alpha} \nabla u \right] dx \\ &+ \int_{\Gamma} \left[\psi (k \nabla \omega) \cdot \mathbf{n}^- + \omega \left(\frac{\partial \mathbf{q}}{\partial \alpha} \cdot \mathbf{n}^- + \frac{\partial \mathbf{q}}{\partial u} \psi \cdot \mathbf{n}^- \right) \right] ds \\ &+ \int_{\Gamma'} \left[\frac{\partial f}{\partial \alpha} + \frac{\partial f}{\partial u} \psi \right] ds \end{aligned} \quad (32)$$

where \mathbf{n}^- is the inward normal [33] and

$$\frac{\partial \mathbf{q}}{\partial \alpha} \cdot \mathbf{n}^- + \frac{\partial \mathbf{q}}{\partial u} \psi \cdot \mathbf{n}^- = \frac{\partial q_N}{\partial \alpha} \quad \text{on } \Gamma_N. \quad (33)$$

To eliminate the unknown state sensitivities ψ , we now solve

$$\nabla \cdot k \nabla \omega = 0 \quad (34)$$

with boundary conditions $\omega_D = 0$ on $\Gamma_D \setminus \Gamma'$ and $q_N^{\omega} = k \nabla \omega \cdot \mathbf{n}^- = 0$ on Γ_N . For the remaining boundary Γ' , we impose

$$\frac{\partial f}{\partial u} + \omega \frac{\partial \mathbf{q}}{\partial u} \cdot \mathbf{n}^- = 0. \quad (35)$$

Since on Γ' we have

$$-\frac{\partial \mathbf{q}}{\partial u} \cdot \mathbf{n}^- = \frac{\partial f}{\partial u} \quad (36)$$

we can substitute (36) into (35) to get

$$\frac{\partial f}{\partial u} - \omega \frac{\partial f}{\partial u} = 0 \quad \text{on } \Gamma' \quad (37)$$

and so the operative boundary condition on Γ' is $\omega_{\Gamma'} = 1$.

References

- [1] Mary P. Anderson, William W. Woessner, and R. J. Hunt. *Applied groundwater modeling: simulation of flow and advective transport*. Academic Press, London ; San Diego, CA, second edition edition, 2015. ISBN 978-0-12-058103-0. OCLC: ocn921253555.
- [2] M.H. Loke, J.E. Chambers, D.F. Rucker, O. Kuras, and P.B. Wilkinson. Recent developments in the direct-current geoelectrical imaging method. *Journal of Applied Geophysics*, 95:135–156, August 2013. ISSN 09269851. doi: 10.1016/j.jappgeo.2013.02.017. URL <https://linkinghub.elsevier.com/retrieve/pii/S0926985113000499>.
- [3] T. Saey, M. Van Meirvenne, P. De Smedt, B. Stichelbaut, S. Delefortrie, E. Baldwin, and V. Gaffney. Combining EMI and GPR for non-invasive soil sensing at the Stonehenge World Heritage Site: the reconstruction of a WW1 practice trench: Reconstructing a practice trench using GPR and EMI. *European Journal of Soil Science*, 66(1):166–178, January 2015. ISSN

13510754. doi: 10.1111/ejss.12177. URL <https://onlinelibrary.wiley.com/doi/10.1111/ejss.12177>.
- [4] Esben Auken, Tue Boesen, and Anders V. Christiansen. A Review of Airborne Electromagnetic Methods With Focus on Geotechnical and Hydrological Applications From 2007 to 2017. volume 58 of *Advances in Geophysics*, pages 47–93. Elsevier, 2017. doi: <https://doi.org/10.1016/bs.agph.2017.10.002>. URL <https://www.sciencedirect.com/science/article/pii/S006526871730002X>. ISSN: 0065-2687.
- [5] Esben Auken, Nikolaj Foged, Jakob Juul Larsen, Knud Valdemar Trøllund Lassen, Pradip Kumar Maurya, Søren Møller Dath, and Tore Tolstrup Eiskjær. tTEM — A towed transient electromagnetic system for detailed 3D imaging of the top 70 m of the subsurface. *GEOPHYSICS*, 84(1):E13–E22, January 2019. ISSN 0016-8033, 1942-2156. doi: 10.1190/geo2018-0355.1. URL <https://library.seg.org/doi/10.1190/geo2018-0355.1>.
- [6] Friedrich Pukelsheim. *Optimal design of experiments*. Number 50 in Classics in applied mathematics. SIAM/Society for Industrial and Applied Mathematics, Philadelphia, classic edition, 2006. ISBN 978-0-89871-604-7. OCLC: ocm62742628.
- [7] Raymond H. Myers, Douglas C. Montgomery, and Christine M. Anderson-Cook. *Response surface methodology: process and product optimization using designed experiments*. Wiley series in probability and statistics. Wiley, Hoboken, New Jersey, fourth edition edition, 2016. ISBN 978-1-118-91601-8.
- [8] D. R. Cox and N. Reid. *The theory of the design of experiments*. Number 86 in Monographs on statistics and applied probability. Chapman & Hall/CRC, Boca Raton, 2000. ISBN 978-1-58488-195-7.
- [9] D. V. Lindley. On a Measure of the Information Provided by an Experiment. *The Annals of Mathematical Statistics*, 27(4):986–1005, December 1956. ISSN 0003-4851. doi: 10.1214/aoms/1177728069. URL <http://projecteuclid.org/euclid.aoms/1177728069>.
- [10] M. C. Shewry and H. P. Wynn. Maximum entropy sampling. *Journal of Applied Statistics*, 14(2):165–170, January 1987. ISSN 0266-4763, 1360-0532. doi: 10.1080/02664768700000020. URL <https://www.tandfonline.com/doi/full/10.1080/02664768700000020>.
- [11] Hossein Mohammadi, Peter Challenor, Daniel Williamson, and Marc Goodfellow. Cross-validation based adaptive sampling for gaussian process models. *arXiv:2005.01814 [stat]*, 2021. URL <https://arxiv.org/abs/2005.01814>. arXiv: 2005.01814.
- [12] Andreas Krause, Ajit Singh, and Carlos Guestrin. Near-Optimal Sensor Placements in Gaussian Processes: Theory, Efficient Algorithms and Empirical Studies. *Journal of Machine Learning Research*, 9(8):235–284, 2008. URL <http://jmlr.org/papers/v9/krause08a.html>.
- [13] Joakim Beck and Serge Guillas. Sequential Design with Mutual Information for Computer Experiments (MICE): Emulation of a Tsunami Model. *SIAM/ASA Journal on Uncertainty Quantification*, 4(1):739–766, January 2016. ISSN 2166-2525. doi: 10.1137/140989613. URL <http://epubs.siam.org/doi/10.1137/140989613>.

- [14] Jonas Moćkus. *Bayesian Approach to Global Optimization: Theory and Applications*. Springer Netherlands, Dordrecht, 1989. ISBN 978-94-009-0909-0. URL <https://doi.org/10.1007/978-94-009-0909-0>. OCLC: 851374758.
- [15] Peter I. Frazier. A Tutorial on Bayesian Optimization. *arXiv:1807.02811 [cs, math, stat]*, July 2018. URL <http://arxiv.org/abs/1807.02811>. arXiv: 1807.02811.
- [16] Artur Souza, Luigi Nardi, Leonardo B. Oliveira, Kunle Olukotun, Marius Lindauer, and Frank Hutter. Bayesian Optimization with a Prior for the Optimum. In Nuria Oliver, Fernando Pérez-Cruz, Stefan Kramer, Jesse Read, and Jose A. Lozano, editors, *Machine Learning and Knowledge Discovery in Databases. Research Track*, pages 265–296, Cham, 2021. Springer International Publishing. ISBN 978-3-030-86523-8.
- [17] Javier Gonzalez, Zhenwen Dai, Philipp Hennig, and Neil Lawrence. Batch bayesian optimization via local penalization. In Arthur Gretton and Christian C. Robert, editors, *Proceedings of the 19th International Conference on Artificial Intelligence and Statistics*, volume 51 of *Proceedings of Machine Learning Research*, pages 648–657, Cadiz, Spain, 09–11 May 2016. PMLR. URL <https://proceedings.mlr.press/v51/gonzalez16a.html>.
- [18] S. Prudhomme and J.T. Oden. On goal-oriented error estimation for elliptic problems: application to the control of pointwise errors. *Computer Methods in Applied Mechanics and Engineering*, 176(1-4):313–331, July 1999. ISSN 00457825. doi: 10.1016/S0045-7825(98)00343-0. URL <https://linkinghub.elsevier.com/retrieve/pii/S0045782598003430>.
- [19] J.T. Oden and S. Prudhomme. Goal-oriented error estimation and adaptivity for the finite element method. *Computers & Mathematics with Applications*, 41(5-6):735–756, March 2001. ISSN 08981221. doi: 10.1016/S0898-1221(00)00317-5. URL <https://linkinghub.elsevier.com/retrieve/pii/S0898122100003175>.
- [20] Ahmed Attia, Alen Alexanderian, and Arvind K Saibaba. Goal-oriented optimal design of experiments for large-scale Bayesian linear inverse problems. *Inverse Problems*, 34(9):095009, September 2018. ISSN 0266-5611, 1361-6420. doi: 10.1088/1361-6420/aad210. URL <https://iopscience.iop.org/article/10.1088/1361-6420/aad210>.
- [21] Nicholas Metropolis, Arianna W. Rosenbluth, Marshall N. Rosenbluth, Augusta H. Teller, and Edward Teller. Equation of State Calculations by Fast Computing Machines. *The Journal of Chemical Physics*, 21(6):1087–1092, June 1953. ISSN 0021-9606, 1089-7690. doi: 10.1063/1.1699114. URL <http://aip.scitation.org/doi/10.1063/1.1699114>.
- [22] W K Hastings. Monte Carlo sampling methods using Markov chains and their applications. *Biometrika*, page 13, 1970.
- [23] Andrew Gelman, editor. *Bayesian data analysis*. Texts in statistical science. Chapman & Hall/CRC, Boca Raton, Fla, 2nd ed edition, 2004. ISBN 978-1-58488-388-3.
- [24] Jun S. Liu. *Monte Carlo Strategies in Scientific Computing*. Springer Series in Statistics. Springer New York, New York, NY, 2004. ISBN 978-0-387-76369-9 978-0-387-

- 76371-2. doi: 10.1007/978-0-387-76371-2. URL <http://link.springer.com/10.1007/978-0-387-76371-2>.
- [25] J. Andrés Christen and Colin Fox. Markov chain Monte Carlo Using an Approximation. *Journal of Computational and Graphical Statistics*, 14(4):795–810, December 2005. ISSN 1061-8600, 1537-2715. doi: 10.1198/106186005X76983. URL <http://www.tandfonline.com/doi/abs/10.1198/106186005X76983>.
- [26] Mikkel B Lykkegaard, Grigorios Mingas, Robert Scheichl, Colin Fox, and Tim J Dodwell. Multilevel Delayed Acceptance MCMC with an Adaptive Error Model in PyMC3. In *Machine Learning for Engineering Modeling, Simulation, and Design Workshop at Neural Information Processing Systems (NeurIPS) 2020*, 2020. https://ml4eng.github.io/camera_ready/04.pdf.
- [27] Mikkel B. Lykkegaard, Tim J. Dodwell, Colin Fox, Grigorios Mingas, and Robert Scheichl. Multilevel Delayed Acceptance MCMC, 2022.
- [28] Tiangang Cui, Colin Fox, and Michael J. O’Sullivan. A posteriori stochastic correction of reduced models in delayed acceptance MCMC, with application to multiphase subsurface inverse problems. *arXiv:1809.03176 [stat]*, September 2018. URL <http://arxiv.org/abs/1809.03176>. arXiv: 1809.03176.
- [29] Heikki Haario, Eero Saksman, and Johanna Tamminen. An Adaptive Metropolis Algorithm. *Bernoulli*, 7(2):223, April 2001. ISSN 13507265. doi: 10.2307/3318737. URL <https://www.jstor.org/stable/3318737?origin=crossref>.
- [30] Hans-Jörg G. Diersch. *FEFLOW: Finite Element Modeling of Flow, Mass and Heat Transport in Porous and Fractured Media*. Springer Berlin Heidelberg, Berlin, Heidelberg, 2014. ISBN 978-3-642-38738-8 978-3-642-38739-5. doi: 10.1007/978-3-642-38739-5. URL <http://link.springer.com/10.1007/978-3-642-38739-5>.
- [31] Hans Petter Langtangen and Anders Logg. *Solving PDEs in Python: The FEniCS Tutorial I*. Number 3 in Simula SpringerBriefs on Computing. Springer International Publishing : Imprint: Springer, Cham, 1st ed. 2016 edition, 2016. ISBN 978-3-319-52462-7. doi: 10.1007/978-3-319-52462-7.
- [32] R.-E. Plessix. A review of the adjoint-state method for computing the gradient of a functional with geophysical applications. *Geophysical Journal International*, 167(2):495–503, November 2006. ISSN 0956540X, 1365246X. doi: 10.1111/j.1365-246X.2006.02978.x. URL <https://academic.oup.com/gji/article-lookup/doi/10.1111/j.1365-246X.2006.02978.x>.
- [33] J. F. Sykes, J. L. Wilson, and R. W. Andrews. Sensitivity Analysis for Steady State Groundwater Flow Using Adjoint Operators. *Water Resources Research*, 21(3):359–371, March 1985. ISSN 00431397. doi: 10.1029/WR021i003p00359. URL <http://doi.wiley.com/10.1029/WR021i003p00359>.
- [34] John L. Wilson and Douglas E. Metcalfe. Illustration and Verification of Adjoint Sensitivity Theory for Steady State Groundwater Flow. *Water Resources Research*, 21(11):1602–1610,

- November 1985. ISSN 00431397. doi: 10.1029/WR021i011p01602. URL <http://doi.wiley.com/10.1029/WR021i011p01602>.
- [35] Ne-Zheng Sun. *Inverse Problems in Groundwater Modeling*, volume 6 of *Theory and Applications of Transport in Porous Media*. Springer Netherlands, Dordrecht, 1999. ISBN 978-90-481-4435-8 978-94-017-1970-4. doi: 10.1007/978-94-017-1970-4. URL <http://link.springer.com/10.1007/978-94-017-1970-4>.
- [36] Zhiming Lu and Velimir V. Vesselinov. Analytical sensitivity analysis of transient groundwater flow in a bounded model domain using the adjoint method. *Water Resources Research*, 51(7): 5060–5080, July 2015. ISSN 0043-1397, 1944-7973. doi: 10.1002/2014WR016819. URL <https://onlinelibrary.wiley.com/doi/abs/10.1002/2014WR016819>.
- [37] Herbert Wang and Mary P. Anderson. *Introduction to groundwater modeling: finite difference and finite element methods*. Series of books in geology. W.H. Freeman, San Francisco, 1982. ISBN 978-0-7167-1303-6.
- [38] Roseanna M. Neupauer and Scott A. Griebing. Adjoint Simulation of Stream Depletion Due to Aquifer Pumping. *Ground Water*, 50(5):746–753, September 2012. ISSN 0017467X. doi: 10.1111/j.1745-6584.2011.00901.x. URL <https://onlinelibrary.wiley.com/doi/10.1111/j.1745-6584.2011.00901.x>.
- [39] Carl Edward Rasmussen and Christopher K. I. Williams. *Gaussian processes for machine learning*. Adaptive computation and machine learning. MIT Press, Cambridge, Mass, 2006. ISBN 978-0-262-18253-9. OCLC: ocm61285753.
- [40] T. J. Dodwell, C. Ketelsen, R. Scheichl, and A. L. Teckentrup. A Hierarchical Multilevel Markov Chain Monte Carlo Algorithm with Applications to Uncertainty Quantification in Subsurface Flow. *SIAM/ASA Journal on Uncertainty Quantification*, 3(1):1075–1108, January 2015. ISSN 2166-2525. doi: 10.1137/130915005. URL <http://epubs.siam.org/doi/10.1137/130915005>.
- [41] M. D. McKay, R. J. Beckman, and W. J. Conover. A comparison of three methods for selecting values of input variables in the analysis of output from a computer code. *Technometrics*, 21(2): 239–245, 1979. ISSN 00401706. URL <http://www.jstor.org/stable/1268522>.
- [42] Pauli Virtanen, Ralf Gommers, Travis E. Oliphant, Matt Haberland, Tyler Reddy, David Cournapeau, Evgeni Burovski, Pearu Peterson, Warren Weckesser, Jonathan Bright, Stéfan J. van der Walt, Matthew Brett, Joshua Wilson, K. Jarrod Millman, Nikolay Mayorov, Andrew R. J. Nelson, Eric Jones, Robert Kern, Eric Larson, C J Carey, İlhan Polat, Yu Feng, Eric W. Moore, Jake VanderPlas, Denis Laxalde, Josef Perktold, Robert Cimrman, Ian Henriksen, E. A. Quintero, Charles R. Harris, Anne M. Archibald, Antônio H. Ribeiro, Fabian Pedregosa, Paul van Mulbregt, and SciPy 1.0 Contributors. SciPy 1.0: Fundamental Algorithms for Scientific Computing in Python. *Nature Methods*, 17:261–272, 2020. doi: 10.1038/s41592-019-0686-2.

- [43] David W. Scott. *Multivariate density estimation: theory, practice, and visualization*. Wiley series in probability and mathematical statistics. Wiley, New York, 1992. ISBN 978-0-471-54770-9.
- [44] N. Chopin. A sequential particle filter method for static models. *Biometrika*, 89(3):539–552, August 2002. ISSN 0006-3444, 1464-3510. doi: 10.1093/biomet/89.3.539. URL <https://academic.oup.com/biomet/article-lookup/doi/10.1093/biomet/89.3.539>.